

# Maximum-Power-Point Tracking Method of Photovoltaic Power System Using Single Transducer

Toshihiko Noguchi, *IEEE, Senior Member*, and Hiroyuki Matsumoto

Nagaoka University of Technology

1603-1 Kamitomioka, Nagaoka 940-2188, Japan  
Phone: +81-258-47-9510, Fax: +81-258-47-9500  
e-mail: tnoguchi@vos.nagaokaut.ac.jp  
URL: pelab.nagaokaut.ac.jp/

**Abstract** — This paper proposes a maximum-power-point tracking (MPPT) method of a photovoltaic power system with less transducer count. A unique feature of this method is capability to seek the maximum power point, using only a single transducer implemented in a switched DC-DC power converter, i.e., a current transducer or a voltage transducer. Output power of the converter can be estimated with an average value and ripple amplitude of the reactor current or the capacitor voltage detected in the converter. The output power obtained from only the current or the voltage information allows seeking the maximum power point on the basis of a common hill-climbing method. In this paper, not only a theoretical aspect of the proposed method is described, but also several experimental results are presented to prove feasibility of the method.

**Index terms:** photovoltaic; maximum-power-point tracking; power estimation; voltage-source DC-DC converter; current-source DC-DC converter.

## I. INTRODUCTION

RESEARCH and development on alternative energy resources to fossil fuels have intensively been promoted due to growing concern on an environmental issue since 1990's. Above all, a photovoltaic power generation system is one of the most promising environment-friendly solutions and has extensively been used by various residential houses, rural power networks, huge commercial power plants and so forth. Photovoltaic power systems are capable to produce electric power with no CO<sub>2</sub> emission and their energy resource is actually infinite, which is the most attractive point. Also, they can easily be installed without very strict restrictions. However, low efficiency and higher cost per unit power are the fatal drawbacks of the systems, which prevents them from being more and widely used, and how to overcome these drawbacks is an important technical issue so far and toward the future.

A technique to utilize the photovoltaic effectively is known as a maximum-power-point tracking (MPPT) method, which makes it possible to acquire as much power as possible from the photovoltaic. Since an electric characteristic of the

output power has a convex property with respect to the operating voltage or current as shown in Fig. 1, there exists only one optimum operating point on the power vs. voltage (or current) curve. The MPPT is a method to let the controller operate at the optimum operating point. There have been various kinds of MPPT methods reported and the most common technique of them is a hill-climbing method, which seeks the optimum operating point by changing the operating point until the maximum power point is found [1]-[4]. Therefore, this method essentially requires power calculation using both the voltage and the current transducers, which should be reduced from a viewpoint of system simplification and cost reduction.

This paper focuses on reduction of the count of such transducers. In order to achieve this goal, either a current ripple or a voltage ripple, which is inherently generated by a switched power converter, is effectively utilized in the proposed system and the output power of the converter is estimated with an average value and ripple amplitude of the current or the voltage detected in the converter. Applying the conventional hill-climbing method to the system, the maximum-power-point can be sought with only a single transducer. The paper discusses a theoretical aspect of the proposed technique, assuming a current-source DC-DC converter or a voltage-source DC-DC converter is employed as an MPPT controller, and presents experimental results to demonstrate excellent MPPT operations of the system.

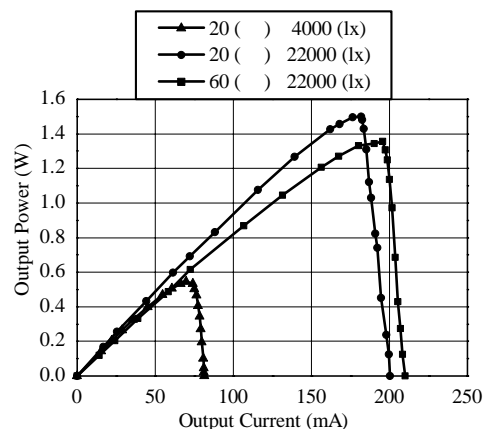


Fig. 1. Example of power vs. current characteristics.

## II. MPPT ALGORITHM WITH SINGLE TRANSDUCER

### A. Power Estimation in Voltage-Source DC-DC Converter

Fig. 2 shows a configuration of the voltage-source DC-DC converter. The system consists of a photovoltaic, a boost chopper with a single current transducer and a load resistor. This circuit operates in switched modes and is regarded as a non-linear system; thus analysis of the circuit is rather complicated. Therefore, a state space averaging method is applied to analyze the circuit operation in order to treat the circuit as a linear system. In the linearization process, the photovoltaic is regarded as an equivalent circuit composed with a DC voltage source  $V_{PV}$  and a series connected internal resistance  $R_{PV}$ , which varies with the operating points, depending on irradiance as well as temperature.

Figs. 3 (a) and 3 (b) show equivalent circuits in an on-mode and an off-mode of the switching device. In these circuits,  $r_L$ ,  $r_S$  and  $r_D$  represent an equivalent resistance that corresponds to losses dissipated in the reactor, an on-mode resistance of the switching device and an equivalent resistance of the diode that corresponds to its forward drop, respectively. The following state variable expression is derived in terms of a capacitor voltage  $v_{C1}$ , a reactor current  $i_L$  and an output voltage  $v_o$  from the equivalent circuit illustrated in Fig. 3 (a) when the switching device is turned on:

$$\frac{dx}{dt} = A_{ON}x + b_{ON}V_{PV}, \quad (1)$$

where

$$A_{ON} = \begin{bmatrix} -\frac{1}{R_{PV}C_1} & -\frac{1}{C_1} & 0 \\ \frac{1}{L} & -\frac{r_L + r_S}{L} & 0 \\ 0 & 0 & \frac{1}{R_L C_2} \end{bmatrix}, \text{ and}$$

$$b_{ON} = \begin{bmatrix} \frac{1}{R_{PV}C_1} & 0 & 0 \end{bmatrix}^T.$$

In a similar manner, when the switching device is turned off, the state variable equation of the converter is expressed as

$$\frac{dx}{dt} = A_{OFF}x + b_{OFF}V_{PV}, \quad (2)$$

where

$$A_{OFF} = \begin{bmatrix} -\frac{1}{R_{PV}C_1} & -\frac{1}{C_1} & 0 \\ \frac{1}{L} & -\frac{r_L + r_D}{L} & -\frac{1}{L} \\ 0 & -\frac{1}{C_2} & \frac{1}{R_L C_2} \end{bmatrix}, \text{ and}$$

$$b_{OFF} = \begin{bmatrix} \frac{1}{R_{PV}C_1} & 0 & 0 \end{bmatrix}^T.$$

In the above equations, the state variable vector is  $x = [v_C \ i_L \ v_o]^T$ . Combining (1) and (2) by using the state space averaging method, an averaged state variable expression can be obtained as follows, where  $\bar{x} = [\bar{v}_C \ \bar{i}_L \ \bar{v}_o]^T$  is an average state variable vector:

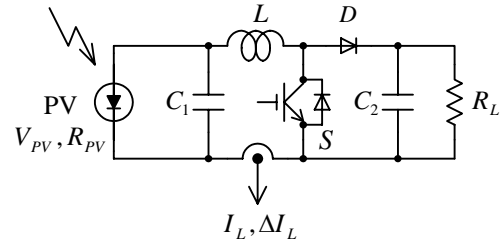


Fig. 2. Photovoltaic and voltage-source DC-DC converter.

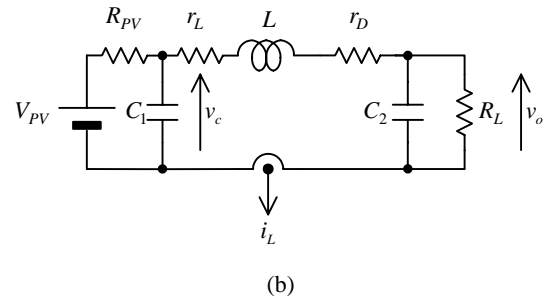
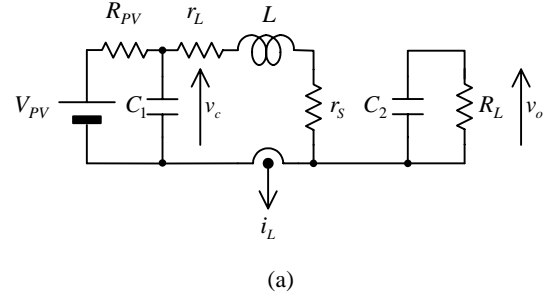


Fig. 3. Equivalent circuits of voltage-source DC-DC converter. (a) On-mode circuit. (b) Off-mode circuit.

$$\frac{d\bar{x}}{dt} = A\bar{x} + bV_{PV}, \quad (3)$$

where

$$A = A_{ON}D + A_{OFF}D'$$

$$= \begin{bmatrix} -\frac{1}{R_{PV}C_1} & -\frac{1}{C_1} & 0 \\ \frac{1}{L} & -\frac{r_L + r_S D + r_D D'}{L} & -\frac{D'}{L} \\ 0 & -\frac{1}{C_2} & \frac{1}{R_L C_2} \end{bmatrix}, \text{ and}$$

$$b = b_{ON}D + b_{OFF}D' = \begin{bmatrix} \frac{1}{R_{PV}C_1} & 0 & 0 \end{bmatrix}^T.$$

In (3),  $D$  and  $D'$  ( $=1-D$ ) are duties of the on-mode and the off-mode of the switching device, respectively.

Since  $d\bar{x}/dt = 0$  in the steady state, the average values of the capacitor voltage  $V_C$ , the reactor current  $I_L$  and the output voltage  $V_o$  can be represented by the following expression:

$$\begin{bmatrix} V_C \\ I_L \\ V_o \end{bmatrix} = \frac{V_{PV}}{r_L + r_S D + r_D D' + R_{PV} + R_L D'^2} * \begin{bmatrix} 1 \\ R_L D' \end{bmatrix}. \quad (4)$$

On the other hand, steady state ripple amplitude of the reactor current  $\Delta I_L$  is expressed as the following equation, which is obtained by making product between (1) and an on-mode time duration:

$$\Delta I_L = \frac{DT_s}{L} \frac{V_{PV}}{r_L + r_S D + r_D D' + R_{PV} + R_L D'^2} * \frac{1}{(r_S D + r_D D' - r_S + R_L D'^2)}, \quad (5)$$

where  $T_s$  is a switching period.

The load power  $W_o$  can be estimated by (4) and (5) as follows, paying attention to that  $V_{PV}$ ,  $R_{PV}$ ,  $V_C$ ,  $V_o$  and  $R_L$  are all unknown variables and constants:

$$W_o = \frac{V_o^2}{R_L} = \frac{L}{DT_s} \Delta I_L I_L + (r_S - r_D) D' I_L^2. \quad (6)$$

It should be noted that  $D$ ,  $D'$  and  $T_s$  are known variables because they are manipulating quantities specified by the controller and that  $L$ ,  $r_S$  and  $r_D$  are circuit parameters of which rough values, e.g., nominal values, are preliminarily available in the circuit design process. Therefore, (6) shows that the output power can be estimated with information of  $I_L$  and  $\Delta I_L$  from only the current transducer.

### B. Power Estimation in Current-Source DC-DC Converter

Fig. 4 shows a schematic diagram of a current-source DC-DC converter, which is known as a Cük converter. The system is composed with a photovoltaic, the Cük converter with a single voltage transducer, i.e., an isolation amplifier, and a load resistor. In the same manner as the voltage-source converter, state variable equations of the current-source converter are represented by the following on-mode and off-mode expressions; in the on-mode as illustrated in Fig. 5 (a),

$$\frac{dx}{dt} = A_{ON}x + b_{ON}V_{PV}, \quad (7)$$

where

$$A_{ON} = \begin{bmatrix} -\frac{R_{PV} + r_{L1} + r_S}{L_1} & -\frac{r_S}{L_1} & 0 & 0 \\ 0 & -\frac{1}{C_1} & 0 & 0 \\ -\frac{r_S}{L_2} & -\frac{r_{L2} + r_S}{L_2} & \frac{1}{L_2} & -\frac{1}{L_2} \\ 0 & \frac{1}{C_2} & 0 & -\frac{1}{C_2 R_L} \end{bmatrix}, \text{ and}$$

$$b_{ON} = \begin{bmatrix} \frac{1}{L_1} & 0 & 0 & 0 \end{bmatrix}^T.$$

Also, in the off-mode shown in Fig. 5 (b),

$$\frac{dx}{dt} = A_{OFF}x + b_{OFF}V_{PV}, \quad (8)$$

where

$$A_{OFF} = \begin{bmatrix} -\frac{R_{PV} + r_{L1} + r_D}{L_1} & -\frac{r_D}{L_1} & -\frac{1}{L_1} & 0 \\ \frac{1}{C_1} & 0 & 0 & 0 \\ -\frac{r_D}{L_2} & -\frac{r_{L2} + r_D}{L_2} & 0 & -\frac{1}{L_2} \\ 0 & \frac{1}{C_2} & 0 & -\frac{1}{C_2 R_L} \end{bmatrix}, \text{ and}$$

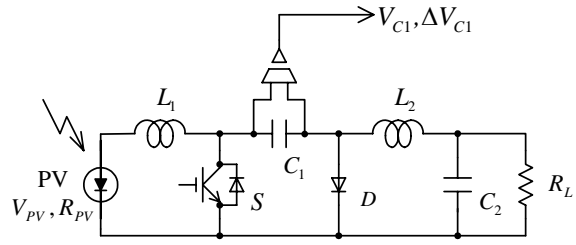
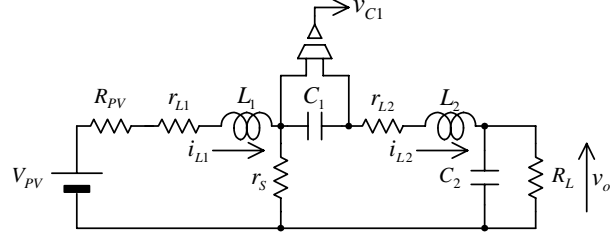
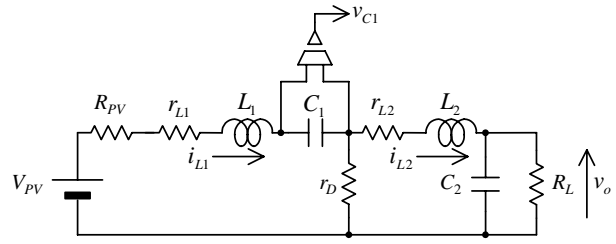


Fig. 4. Photovoltaic and current-source DC-DC converter.



(a)



(b)

Fig. 5. Equivalent circuits of current-source DC-DC converter. (a) On-mode circuit. (b) Off-mode circuit.

$$b_{OFF} = \begin{bmatrix} \frac{1}{L_1} & 0 & 0 & 0 \end{bmatrix}^T.$$

In the above equations, the state variable vector is defined as  $x = [i_{L1} \ v_{C1} \ i_{L2} \ v_o]^T$  where  $i_{L1}$ ,  $v_{C1}$ ,  $i_{L2}$  and  $v_o$  are a current of the reactor  $L_1$ , a voltage across the capacitor  $C_1$ , a current of the reactor  $L_2$  and the output voltage, respectively. Therefore, the following expression can be derived on the basis of the state space averaging method, where  $\bar{x} = [\bar{i}_{L1} \ \bar{v}_{C1} \ \bar{i}_{L2} \ \bar{v}_o]^T$  denotes an average state variable vector of the converter:

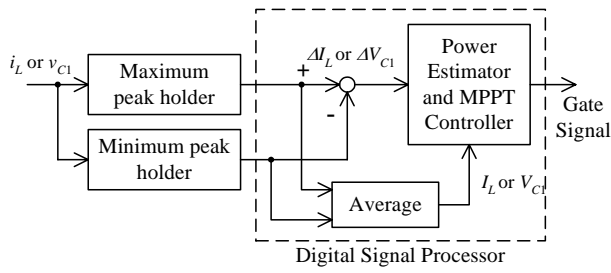
$$\frac{d\bar{x}}{dt} = A\bar{x} + bV_{PV}, \quad (9)$$

where

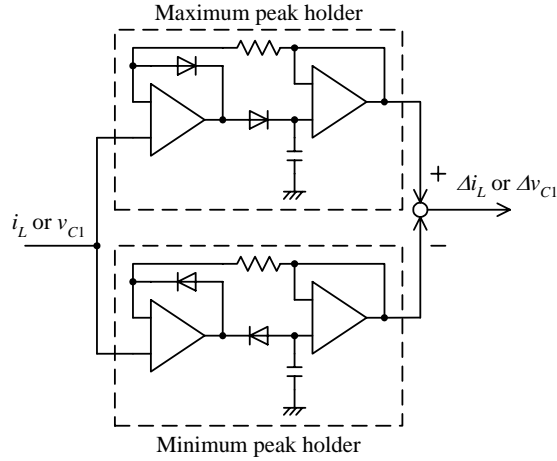
$$A = A_{ON}D + A_{OFF}D'$$

$$= \begin{bmatrix} -\frac{R_{PV} + r_{L1} + r_S D + r_D D'}{L_1} & -\frac{r_S D + r_D D'}{L_1} & -\frac{D'}{L_1} & 0 \\ \frac{D'}{C_1} & -\frac{D}{C_1} & 0 & 0 \\ -\frac{r_S D + r_D D'}{L_2} & -\frac{r_{L2} + r_S D + r_D D'}{L_2} & \frac{D}{L_2} & -\frac{1}{L_2} \\ 0 & \frac{1}{C_2} & 0 & -\frac{1}{C_2 R_L} \end{bmatrix},$$

$$\text{and } b = b_{ON}D + b_{OFF}D' = \begin{bmatrix} \frac{1}{L_1} & 0 & 0 & 0 \end{bmatrix}^T.$$



(a)



(b)

Fig. 6. Block diagram of proposed MPPT controller. (a) Configuration of whole controller. (b) Detailed schematic of ripple amplitude detector.

Average values of the state variables in the steady state are obtained by substituting  $d\bar{x}/dt=0$  into (9) as described in (10):

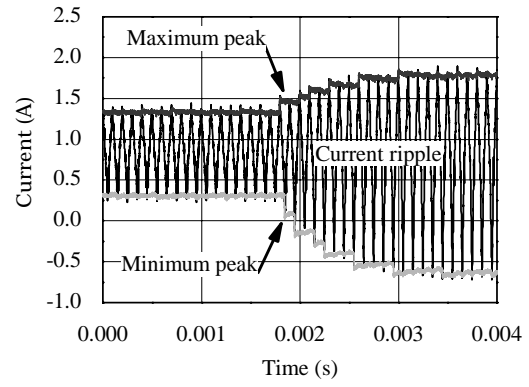
$$\begin{bmatrix} I_{L1} \\ V_{C1} \\ I_{L2} \\ V_o \end{bmatrix} = \frac{V_{PV}}{(R_{PV} + r_{L1})D^2 + r_s D + (R_L + r_{L2})D'^2 + r_D D'} * \begin{bmatrix} D^2 \\ r_s D + (r_D + r_{L2} + R_L)D' \\ DD' \\ R_L DD' \end{bmatrix}. \quad (10)$$

Also, steady state ripple amplitude of the capacitor voltage  $\Delta V_{C1}$  is given by the following equation:

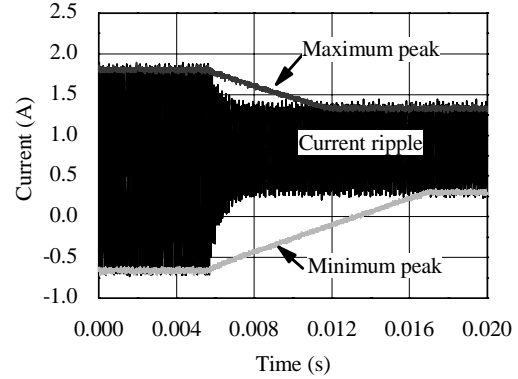
$$\Delta V_{C1} = \frac{D^2 D' T_s}{C_1} * \frac{V_{PV}}{(R_{PV} + r_{L1})D^2 + r_s D + (R_L + r_{L2})D'^2 + r_D D'}. \quad (11)$$

Canceling out the unknown variables and constants, i.e.,  $V_{PV}$ ,  $R_{PV}$ ,  $I_{L1}$ ,  $I_{L2}$  and  $R_L$ , from (10) and (11), the output power  $W_o$  can be estimated only with  $V_{C1}$  and  $\Delta V_{C1}$  from the voltage transducer as follows:

$$W_o = \frac{V_o^2}{R_L} = C_1 \frac{\Delta V_{C1}}{T_s} V_{C1} - \frac{r_s D + (r_D + r_{L2})D'}{D'} \left( C_1 \frac{\Delta V_{C1}}{DT_s} \right)^2. \quad (12)$$



(a)



(b)

Fig. 7. Responses of peak holders. (a) Response in case of increasing ripple. (b) Response in case of decreasing ripple.

### III. EXPERIMENTAL SETUP AND RESULTS

#### A. Configuration of Single Transducer Based MPPT System

Fig. 6 shows system configuration of the proposed MPPT controller. The controller requires current detection with a Hall-effect CT or voltage detection with an isolation amplifier in order to estimate the output power by (6) or (12). According to (6) and (12), both of the maximum and the minimum peak values of the reactor current or the capacitor voltage must be detected to calculate the ripple amplitude of the current or the voltage. Also, an average value of the reactor current or the capacitor voltage can be calculated from the maximum and the minimum peak values detected.

It is requisite to sample the reactor current or the capacitor voltage synchronously with a switching pattern of the converter because the maximum and the minimum peak values are detected at rising edges and falling edges of the pattern. However, this approach demands sophisticated A/D converters with high-sampling rate and high-resolution, which is a disadvantage from a viewpoint of circuit implementation and cost. In order to overcome this difficulty, a simple OP-amp based analog circuit is employed in the proposed system as shown in Fig. 6 (b), which is an external front-end of the A/D converters embedded in a digital signal processor. The ripple amplitude of the reactor current  $\Delta I_L$  or the ripple

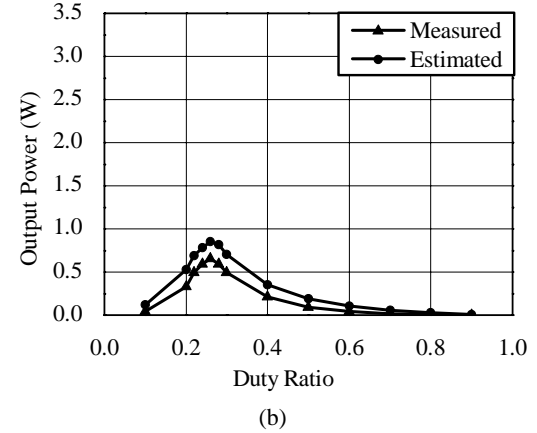
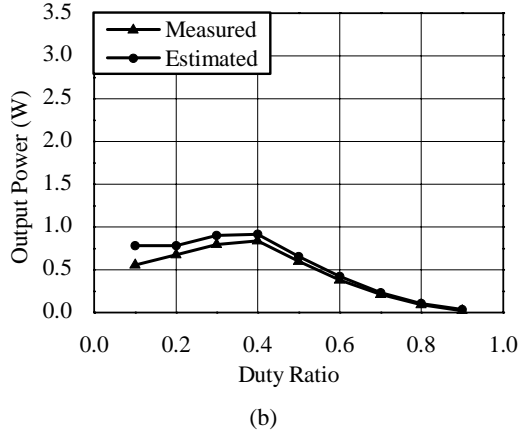
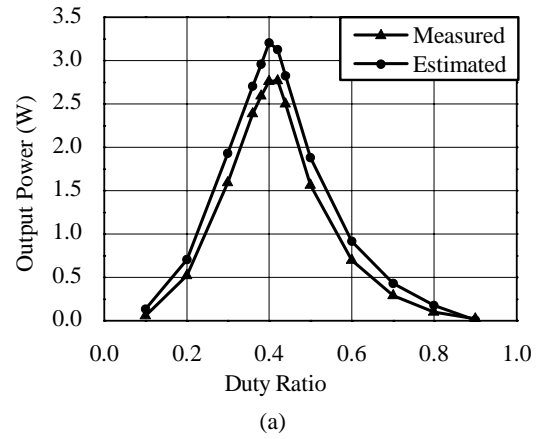
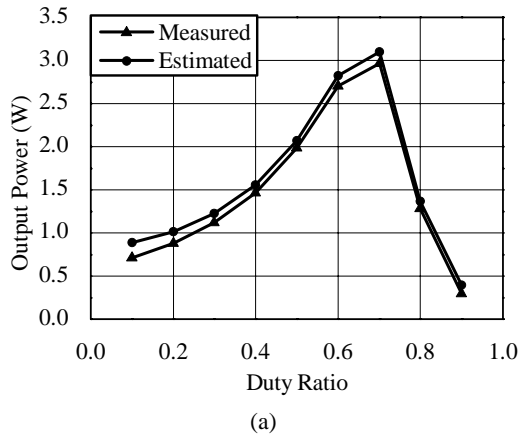


Fig. 8. Comparison between measured and estimated power of voltage-source DC-DC converter with single current transducer. (a) Irradiance: 2.43 (kW/m<sup>2</sup>). (b) Irradiance: 1.06 (kW/m<sup>2</sup>).

Fig. 9. Comparison between measured and estimated power of current-source DC-DC converter with single voltage transducer. (a) Irradiance: 2.43 (kW/m<sup>2</sup>). (b) Irradiance: 1.06 (kW/m<sup>2</sup>).

amplitude of the capacitor voltage  $\Delta V_{C1}$  is calculated from difference between the maximum and the minimum peak values, while the average reactor current  $I_L$  or the average capacitor voltage  $V_{C1}$  is obtained from the sum of the both peak values.

### B. Operation of Ripple Amplitude Detector

Figs. 7 (a) and 7 (b) show tracking characteristics of the ripple amplitude detector when the ripple amplitude of a test signal is changed stepwise. Fig. 7 (a) corresponds to the case of increased amplitude and Fig. 7 (b) is the case of decreasing. As can be seen in Fig. 7 (a), the ripple amplitude detector properly tracks the step changes of the ripple without large delays. However, Fig. 7 (b) indicates that it takes approximately 8 (ms) and 14 (ms) for the ripple amplitude detector to track new maximum and minimum values, respectively. These delays are caused by discharge time constant of the capacitors in the OP-amp circuit. However, these delays hardly affect MPPT performance of the system because solar irradiation does not vary in a few milliseconds.

### C. Evaluation of Estimated Power from Single Transducer

Several experimental tests were conducted to examine estimation performance of the proposed method under a test

condition listed in TABLE I. Fig. 8 shows experimental results of the voltage-source DC-DC converter and comparison between the measured output power and the estimated one by (6) from current transducer information. Small error can be observed in a low-duty range but the estimated output power conforms to the measured power very well both in a higher irradiance condition and in a lower irradiance condition. Fig. 8 (a) indicates that the maximum power points of the estimated and the measured results are observed commonly at  $D=0.70$ , while the both maximum power points can be seen at  $D=0.40$  in Fig. 8 (b).

Fig. 9 shows similar characteristics of the current-source DC-DC converter and comparison between experimental results of the measured and the estimated output power by (12). It is confirmed that the estimated values are slightly larger than measured values in a whole range of the duty ratio. However, the estimated power reaches the maximum power point at  $D=0.42$  similarly with the measured one as shown in Fig. 9 (a), while Fig.9 (b) shows that the maximum power points of both data are observed at  $D=0.26$ .

Since the optimum operating points are sought by a common hill-climbing method as described before, absolute accuracy in estimating the output power is not important to achieve accurate MPPT operation. In other words, it is

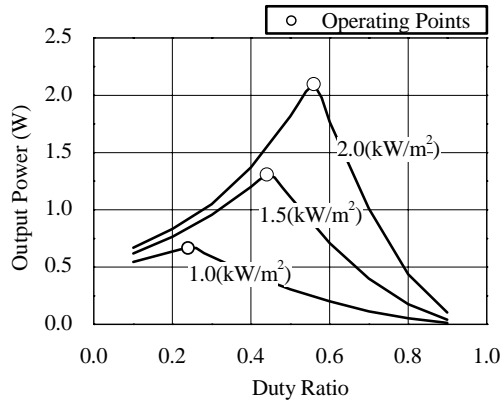


Fig. 10. Output power vs. duty ratio characteristics and operating points of voltage-source DC-DC converter with single current transducer.

TABLE I EXPERIMENTAL CONDITIONS

Test photovoltaic	GL418-TF
Rated maximum power	6.5 (W)
Rated output voltage	6 (V)
Panel surface temperature	50 (°C)
Switching frequency	10 (kHz)

possible to seek the maximum power point accurately as far as both the estimated and the measured curves have their peaks at the same duty ratio.

#### D. Discussion on Estimation Error

As can be seen in Fig. 8 (in the case of the voltage-source DC-DC converter), the estimation error slightly increases in a low-duty range. It is inferred that calculation error in (6) is dominant cause of the estimation error because the denominator of the first term in (6) is detrimentally affected by the duty ratio in the low-duty range. Therefore, the estimation error increases as the duty ratio is reduced if the current detection error is always constant.

On the other hand, in the case of the current-source DC-DC converter, almost constant estimation error, which looks independent of the duty ratio, can be seen in Fig. 9. In this case, the estimation algorithm is expressed by (12) and its principal term, i.e. the first term, does not include the duty. This is the reason why the estimation error is hardly affected by the duty ratio. It is a detection error of the voltage or a parameter mismatch of the capacitor rather than the duty ratio that degrades the estimation characteristic.

#### E. Experimental Results of MPPT Operation

The MPPT operation was carried out by adopting a common hill-climbing method to the proposed system. Figs. 10 and 11 show the experimental results of the voltage-source DC-DC converter and the current-source DC-DC converter, respectively. As can be seen in these figures, the MPPT operation was properly performed in both converters and their operating points were placed close to the maximum power

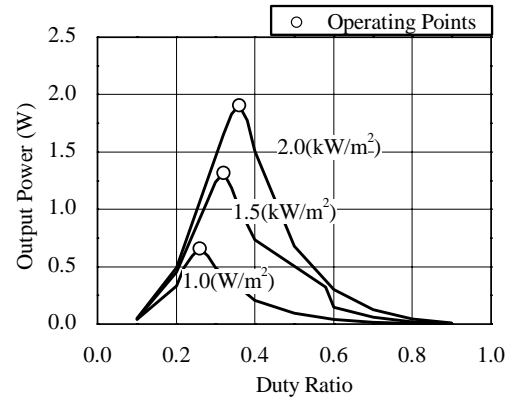


Fig. 11. Output power vs. duty ratio characteristics and operating points of current-source DC-DC converter with single voltage transducer.

points even though irradiance widely changed. A tracking error, which was a deviation of the operating point from the real maximum power point, was within 4 % with respect to the duty ratio. Therefore, the proposed single transducer approach is quite effective to make an accurate MPPT possible.

#### IV. CONCLUSION

This paper has discussed a novel strategy of an MPPT operation of a photovoltaic power system with less transducer count in power converters. The proposed strategy allows output power estimation with only a single current transducer or a single voltage transducer. Theoretical analysis of this approach has been developed on two types of converters, i.e., the voltage-source DC-DC converter and the current-source DC-DC converter. Also, a practical implementation technique to estimate the output power has been presented, which allows a simple circuit configuration without sacrificing accuracy of the power estimation. Two types of experimental systems have been setup and proper estimation characteristics have been confirmed through several experimental tests. Consequently, an excellent tracking performance to the maximum-power-points has been confirmed with sufficient accuracy, using only a single transducer.

#### REFERENCES

- [1] O. Wasynczuk, "Dynamic Behavior of a Class of Photovoltaic Power Systems," *IEEE Trans. on Power Appl. Sys.*, vol. **102**, no. 9, pp. 3031-3037, 1983.
- [2] Katsumi Ohniwa, and Tsuyoshi Sato, "A Simplified Maximum Power Tracking Method for Photovoltaic Solar System," *IEE-Japan Trans. on Power Sys.*, vol. **106-B**, no. 7, pp. 72-78, 1984.
- [3] C. Hua, J. Lin, and C. Shen, "Implementation of a DSP-Controlled Photovoltaic System with Peak Power Tracking," *IEEE Trans. on Ind. Elec.*, vol. **45**, no. 1, pp. 99-107, 1998.
- [4] K. Takahara, and T. Matsuda, "An Adaptive Control Method for Maximum Power Tracking of Photovoltaic Power Generator," *IEE-Japan Trans. on Ind. Appl.*, vol. **118-D**, no. 6, pp. 810-811, 1998.